

## Proton Radioactivity Measurements at HRIBF: Ho, Lu, and Tm Isotopes

C. R. Bingham,<sup>1,2</sup> J. C. Batchelder,<sup>3</sup> K. Rykaczewski,<sup>2,4</sup> K. S. Toth,<sup>2</sup> Y. Akovali,<sup>2</sup> T. Davinson,<sup>5</sup> T. N. Ginter,<sup>6</sup> C. J. Gross,<sup>2,7</sup> R. Grzywacz,<sup>1</sup> J. H. Hamilton,<sup>6</sup> Z. Janas,<sup>4</sup> M. Karny,<sup>4</sup> S. H. Kim,<sup>1</sup> B. D. MacDonald,<sup>8</sup> J. F. Mas,<sup>2</sup> J. W. McConnell,<sup>2</sup> A. Piechaczek,<sup>9</sup> J. J. Ressler,<sup>10</sup> R. C. Slinger,<sup>5</sup> J. Szerypo,<sup>11</sup> W. Weintraub,<sup>1</sup> P. J. Woods,<sup>5</sup> C. -H. Yu,<sup>2</sup> and E. F. Zganjar<sup>8</sup>

<sup>1</sup>Department of Physics, University of Tennessee, Knoxville, TN 37996, USA  
E-Mail: cbingham@utk.edu

<sup>2</sup>Physics Division, Oak Ridge National Laboratory, Oak Ridge, TN 37831, USA

<sup>3</sup>UNIRIB/Oak Ridge Institute for Science and Education, Oak Ridge, TN 37831, USA

<sup>4</sup>IEP, Warsaw University, 00681 Warsaw, Hoza 69, POLAND

<sup>5</sup>University of Edinburgh, EH9 3JZ, UNITED KINGDOM

<sup>6</sup>Department of Physics, Vanderbilt University, Nashville, TN 37235, USA

<sup>7</sup>Oak Ridge Institute for Science and Education, Oak Ridge, TN 37831, USA

<sup>8</sup>Department of Physics, Georgia Institute of Technology, Atlanta, GA 30332, USA

<sup>9</sup>Department of Physics, Louisiana State University, Baton Rouge, LA 70803, USA

<sup>10</sup>Department of Chemistry, University of Maryland, College Park, MD 20742, USA

<sup>11</sup>Joint Institute for Heavy Ion Research, Oak Ridge, TN 37831, USA

Two new isotopes, <sup>145</sup>Tm and <sup>140</sup>Ho and three isomers in previously known isotopes, <sup>141m</sup>Ho, <sup>150m</sup>Lu and <sup>151m</sup>Lu have been discovered and studied via their decay by proton emission. These proton emitters were produced at the Holifield Radioactive Ion Beam Facility (HRIBF) by heavy-ion fusion-evaporation reactions, separated in A/Q with a recoil mass spectrometer (RMS), and detected in a double-sided silicon strip detector (DSSD). The decay energy and half-life was measured for each new emitter. An analysis in terms of a spherical shell model is applied to the Tm and Lu nuclei, but Ho is considerably deformed and requires a collective model interpretation.

### 1 Introduction

Proton emission from the nuclear ground state only occurs for nuclei having a significantly negative proton separation energy. The measurement of the proton energy gives a direct test of mass formulas at the limits of nuclear existence and enables improvements to the models. The proton must have sufficient energy to tunnel through the Coulomb barrier, and the orbital angular momentum barrier if it is not an  $l = 0$  proton. The Coulomb barrier is proportional to the charge of the tunneling particle, while the orbital angular momentum term is inversely proportional to the mass. Consequently, the orbital angular momentum part is relatively more important in determining

RECEIVED  
MAR 25 1999  
OSTI

## **DISCLAIMER**

**Portions of this document may be illegible in electronic image products. Images are produced from the best available original document.**

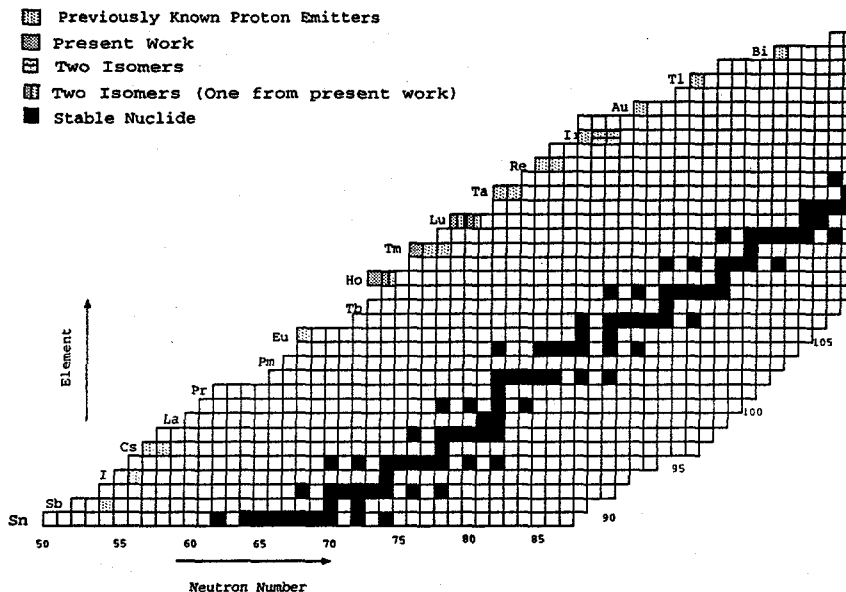


Figure 1: A Portion of the Chart of Nuclides Where the Known Ground-State and Low-Lying Isomeric Proton Emitters Lie. The known proton emitters are shaded with the five reported in the present paper highlighted, while for reference, the stable nuclides are blackened.

the decay rate for proton radioactivity than for  $\alpha$  decay. For this reason, it is usually possible to identify the orbital angular momentum of the emitted proton, and thus, for regions where the spherical shell model is appropriate, the shell model wave function can be investigated.

The proton radioactivity of a nuclear ground state was first observed in 1981, when the decay of  $^{151}\text{Lu}$  was measured.<sup>1</sup> The observation of other cases was rather slow in developing, primarily due to the need for heavy-ion accelerators coupled to on-line recoil mass spectrometers to produce and rapidly separate nuclei far from stability. Also, in recent years the development of double-sided silicon strip detectors (DSSD)<sup>2</sup> has aided in the rapid detection and identification of these short-lived proton emitters. In the last several years, the number of known emitters was increased significantly, primarily due to the use of DSSDs at the exit of the Fragment Mass Analyzer (FMA) at Argonne. With the restart of the Holifield Facility (HRIBF) and the commissioning of the new Recoil Mass Spectrometer,<sup>3</sup> a strip detector set-up was developed at HRIBF and used to add 5 cases to the known ground-state and isomeric proton emitters. The total number of such known emitters is now about 30. With

Table 1: Details on the Reactions, Beams, and Targets Used to Produce the Proton Emitters Reported.

Product	Reaction	Beam	Target
		Energy (MeV)	Thickness (mg/cm <sup>2</sup> )
<sup>140</sup> Ho	<sup>92</sup> Mo( <sup>54</sup> Fe,p5n) <sup>140</sup> Ho	315	0.91
<sup>141</sup> Ho	<sup>92</sup> Mo( <sup>54</sup> Fe,p4n) <sup>141</sup> Ho	315	0.91
<sup>145</sup> Tm	<sup>92</sup> Mo( <sup>58</sup> Ni,p4n) <sup>145</sup> Tm	315	0.91
<sup>150</sup> Lu	<sup>96</sup> Rb( <sup>58</sup> Ni,p3n) <sup>150</sup> Lu	292	0.54
<sup>151</sup> Lu	<sup>96</sup> Rb( <sup>58</sup> Ni,p2n) <sup>151</sup> Lu	266	0.54

the exception of <sup>53</sup>Co, which has a known high-spin isomer which decays by proton emission,<sup>4</sup> all of the known emitters lie above Sn on the periodic chart. This part of the chart is shown in Fig. 1, where the known proton emitters are highlighted.

## 2 Experimental Method and Details

The experiments utilized <sup>54</sup>Fe and <sup>58</sup>Ni beams from the HRIBF tandem accelerator to produce the exotic nuclei of interest. The beam energies and details about the target for each new isotope studied are given in Table 1. The fusion-evaporation residues were separated from the beam and dispersed in A/Q at the focal plane of the RMS. A position sensitive avalanche counter (PSAC) at the focal plane was used to select the correct mass to implant in the double-sided silicon strip detector (DSSD) which was located behind the PSAC. The detector was about 60 μm thick and had a surface area of 4cm × 4cm and was separated into 1600 pixels by 40 vertical strips on the front and 40 horizontal strips on the back, each of which was monitored to determine the location (pixel) of each implant or decay. The detector surface was large enough to intercept the entire locus of one mass and about 1/2 of the recoils of one neighboring mass. Charges collected from the 80 strips were fed to charge sensitive preamplifiers for processing. Because of the large difference in the implant energies (limited by absorbers to about 30 to 40 MeV) and the protons of interest (~ 1 MeV), the preamp signals were split to feed both implant amplifiers (with 200 MeV dynamic range) and decay amplifiers (with 20 MeV dynamic range). However, the presence of the implant signals in the decay amplifiers produced saturation which required at least 5 μs to clear and thus, produced a limitation on how quickly one could observe a decay event occurring after the implant. The fast decay events appear on the tail of the saturated implant pulses resulting in poorer energy resolution for short-lived

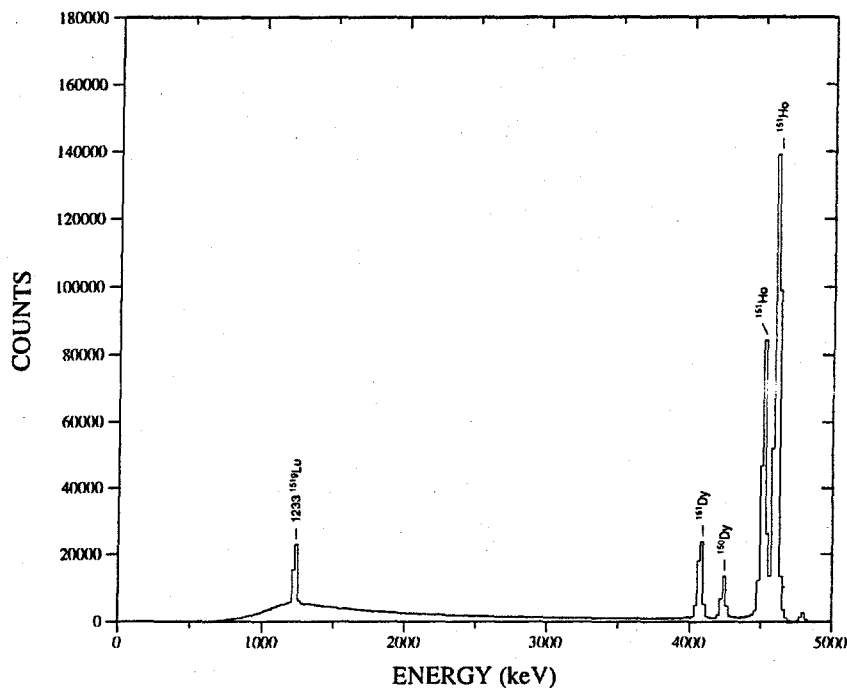


Figure 2: Spectrum of charged particles emitted by mass 151 and 150 recoils in the first 500 ms after implantation.

emitters.

The clock time and pixel were recorded for each implant event, defined as a coincidence between the PSAC and the DSSD. The clock time, pixel, and particle energy were recorded for each decay event, defined as a DSSD without a corresponding PSAC signal. The time between the arrival of an implant in a particular pixel and the next decay in that pixel was used to determine the half-life of proton and  $\alpha$  emitters produced in the experiment.

### 3 Experimental Results

#### 3.1 Proton Radioactivity in $^{150,151}\text{Lu}$

Lu-151 was the first case of observed proton radioactivity from a nuclear ground state,<sup>1</sup> although the proton radioactivity of a high-spin isomer in  $^{53}\text{Co}$  had been observed earlier.<sup>4</sup> Contrary to other proton-emitting nuclei in the mass-

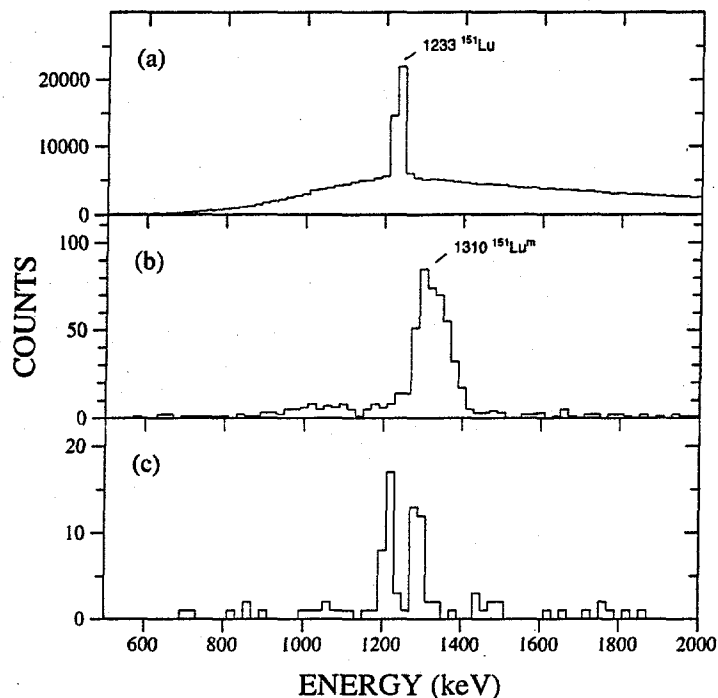


Figure 3: Charged particle spectra at mass 151 with various time constraints: (a) decays occurring within 400 ms of the implant, (b) decays occurring within 50  $\mu$ s of an implant, and (c) decays occurring between 50 and 250  $\mu$ s after an implant. Part (c) clearly shows two proton peaks arising from decay of the  $^{151}\text{Lu}$  ground state and the newly discovered  $^{151}\text{Lu}$  isomer.

150 region where both  $h_{11/2}$  ground states and  $d_{3/2}$  (or  $s_{1/2}$ ) isomeric states have been seen to decay by proton emission,<sup>5</sup> only the  $h_{11/2}$  ground state was observed in  $^{151}\text{Lu}$ . Therefore, we undertook to study the nucleus again, taking care to observe decays in the microsecond half-life range, to locate the low-spin isomer and measure its half-life.

The particle spectrum up to 5 MeV obtained at mass 151 (with a bit of mass 150 also on the detector) is shown in Fig. 2. The strong  $\alpha$  peaks appear above 4 MeV, but there is also a continuum of alphas at lower energies due to those which escaped through the front of the detector and hence deposited only a portion of their energy. The peak at 1.233 MeV is due to the proton decay of the  $^{151}\text{Lu}$  ground state observed earlier.<sup>1</sup> From the present data, a half-life of 80(2) ms was determined for the  $^{151}\text{Lu}$  ground state. The region of the spectrum near this proton peak is replotted in Fig. 3 with constraints on

the correlation time between the implant in the detector and the subsequent decay. Part (a), with a 400 ms constraint, shows primarily the ground-state proton line sitting on the background of escape  $\alpha$  particles. Part (b), with a 50  $\mu$ s constraint reveals another peak at slightly higher energy which decays much more rapidly than the ground state peak and is assigned to the decay of an isomer in  $^{151}\text{Lu}$ . Part (c) was constructed with a time window which permitted a portion of both these lines to be present and minimized poor resolution effects near implantation times; it was used to determine the energy of the isomeric proton to be 1310(10) keV. The half-life of the new isomer was measured to be 16(1)  $\mu$ s.

In another bombardment  $^{150}\text{Lu}$  was produced and studied in a similar manner. The statistics were not as good for this case and hence the experimental values are less accurate. The previously known ground-state proton<sup>5</sup> at 1.26 MeV was observed and the half-life remeasured to be 48.6(4.7) ms. A new isomer with proton energy 1.29(3) MeV was determined to have a half-life of  $33^{+35}_{-12}\mu\text{s}$ .

### 3.2 New Isotope: $^{145}\text{Tm}$

The proton emission from  $^{145}\text{Tm}$ , the first studied with the new strip detector set-up at the back of the RMS at HRIBF, was previously reported.<sup>6</sup> The energy of the proton is 1.728(10) MeV and the half-life was determined to be 3.5(10)  $\mu$ s. This is the shortest half-life of a ground-state proton emitter that has been measured to date.

### 3.3 New Ho Proton Emitters

Some sample spectra resulting from the bombardment of  $^{92}\text{Mo}$  with 315-MeV  $^{54}\text{Fe}$  are shown in Fig. 4. The central panel has a mass cut on 141 and displays particles that were emitted within 25 ms of an implant. The peak at 1169(8) keV decays with a half-life of 3.9(5) ms and was identified earlier.<sup>7</sup> The top panel also emphasizes mass 141 recoils, but has a tighter time limitation; the particle must be emitted within 200  $\mu$ s of an implant. The peak at 1230(20) keV decays with a half-life of 8(3)  $\mu$ s, and is identified with the proton decay of an isomer in  $^{141}\text{Ho}$ . The bottom panel displays decays that occur within 25 ms, but with a mass cut to emphasize the 140 products; due to the fact that the mass peaks overlap a bit, some  $^{141}\text{Ho}$  protons appear in the spectrum, but a new peak at 1086(10) keV decays with a half-life of 6(3) ms and is identified with the decay of  $^{140}\text{Ho}$ .

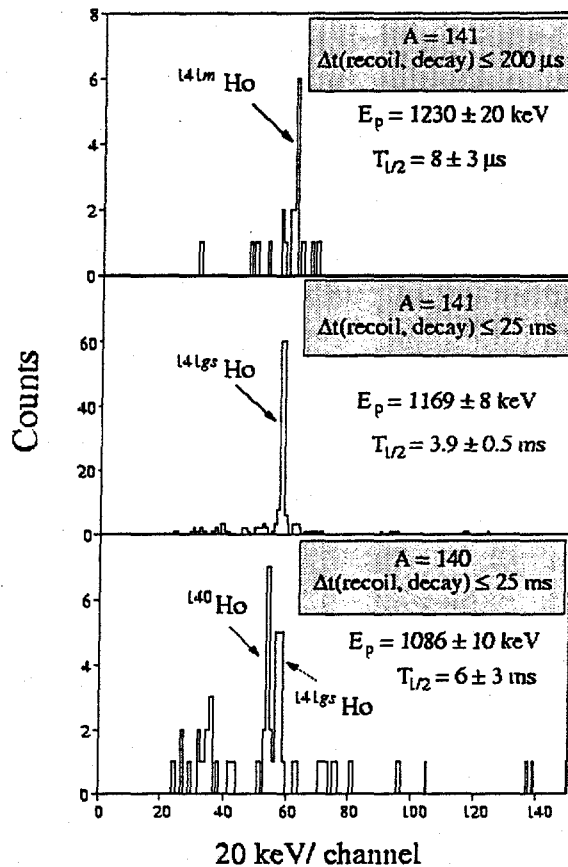


Figure 4: Spectra taken under different mass and time conditions.

#### 4 Comparison with Calculations and Discussion

The results for the five new proton emitters reported here are listed in Table 2. The calculated half-lives were determined with the WKB approximation using the prescription of Hofmann,<sup>8</sup> which utilizes the proton potential of Becchetti and Greenlees.<sup>9</sup> The shell-model orbitals filling between  $Z = 64$  and  $82$  are the  $h_{11/2}$ ,  $d_{3/2}$ , and  $s_{1/2}$  states and hence, calculations were made for each of these possibilities. From the comparison of the calculations with the experimental half-lives, it is obvious that the new isomers in  $^{150,151}\text{Lu}$  are  $I^\pi = 3/2^+$  states, although the calculated half-lives are somewhat shorter than the measured ones. For  $^{145}\text{Tm}$ , the measured half-life agrees fairly well with the calculated one for the  $h_{11/2}$  state. It is noted that the measured half-life for  $^{140}\text{Ho}$  is much



Table 2: Summary of the Experimental Proton Energies and Half-Lives in Comparison with WKB Approximation Calculations of the Half-lives with Different Possible Orbitals of the Valence Proton.

Isomer	$E_p(\text{MeV})$	Exp $t_{1/2}$ ( $\mu\text{s}$ )	Calculated $t_{1/2}$ ( $\mu\text{s}$ )		
			$h_{11/2}$	$d_{3/2}$	$s_{1/2}$
$^{140}\text{Ho}$	1.086(10)	6000(3000)	$32(9) \times 10^4$	81(24)	8(2)
$^{141m}\text{Ho}$	1.169(8)	8(3)	$32(7) \times 10^3$	8.6(18)	0.89(18)
$^{145}\text{Tm}$	1.728(10)	3.5(10)	$1.8^{+0.3}_{-0.2}$	0.0007(1)	$8.0(12) \times 10^{-5}$
$^{150m}\text{Lu}$	1.290(30)	$33^{+35}_{-12}$	$19000^{+20000}_{-9000}$	$7^{+7}_{-3}$	$0.8^{+0.8}_{-0.4}$
$^{151m}\text{Lu}$	1.310(15)	16(1)	11000(4000)	$4.2^{+1.8}_{-1.2}$	$0.48^{+0.20}_{-0.14}$

larger than the WKB calculated values for  $d_{3/2}$  and  $s_{1/2}$  orbitals and less than the  $h_{11/2}$  value by a factor of 50. This is indicative of the large deformation of nuclei in this region as predicted by the model of Möller and Nix.<sup>10</sup> While the isomeric half-life in  $^{141}\text{Ho}$  is close to the  $d_{3/2}$  value, the ground state half-life does not agree with a simple interpretation, and indeed, has already been used to show that  $^{141}\text{Ho}$  has a large deformation.<sup>7</sup>

Recently, the semiclassical WKB method was re-investigated<sup>11</sup> along with more realistic calculations with the DWBA and the two-potential approach (TPA) of Gurvitz and Kalbermann.<sup>12,13</sup> In general the semiclassical WKB approach gives half-lives in good agreement with the other methods. None of these calculations include nuclear structure information, and the experimental spectroscopic factor  $S_p^{exp}$  is defined as the ratio of the calculated and experimental half-lives

$$S_p^{exp} = t_{1/2}^{calc} / t_{1/2}^{exp}.$$

As explained in Ref. <sup>11</sup> these experimental values may be compared with spectroscopic factors from various nuclear models. For the spherical shell model, the independent-quasiparticle approximation (BCS) can be used to deduce

$$S_p^{th} = u_j^2,$$

where  $u_j^2$  is the probability that the spherical orbital ( $nlj$ ) is empty in the daughter nucleus.

In Fig. 5 the spectroscopic factors from the present work are plotted along with other values in the subshell between  $Z = 64$  and  $82$  and compared with theoretical values.<sup>11</sup> It is observed that the single-particle shell-model predictions in this region are in reasonable agreement with the experimental values for  $h_{11/2}$  and  $s_{1/2}$  states. However, the experimental  $d_{3/2}$  spectroscopic factors are seen to be systematically smaller than the shell-model values except

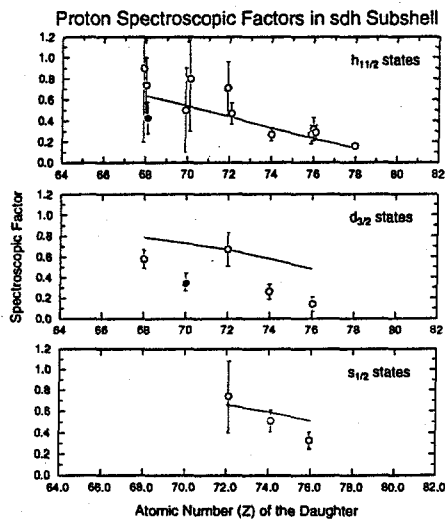


Figure 5: Comparison of experimental (dots) and theoretical (lines) spectroscopic factors for the region with  $64 < Z < 82$  for  $h_{11/2}$ ,  $d_{3/2}$ , and  $s_{1/2}$  states. The present spectroscopic factors are shown as solid points and the other data were taken from Ref. <sup>11</sup> and references therein.

for  $^{156}\text{Ta}$ , indicating that the  $3/2^+$  states have more configurations with which to mix, and hence only a portion of the total  $d_{3/2}$  single-particle configuration is present in the lowest  $3/2^+$  state. For example, in a weak-coupling model, one could devise another low-lying  $3/2^+$  state by coupling a  $s_{1/2}$  proton to the first  $2^+$  level of the daughter. If we consider a two level mixing model composed of  $\pi d_{3/2}$  and  $\pi s_{1/2} \otimes < 2^+ >$  components, the first of these would decay to the  $0^+$  ground state of the daughter while the second would not easily proton-decay to the ground state. The fact that our experimental spectroscopic factor is about half the expected single particle value for a  $d_{3/2}$  state supports about equal amplitudes for the two components in this model.

#### Acknowledgments

Nuclear physics research at The University of Tennessee, Vanderbilt University, and Georgia Institute of Technology is supported by the U. S. Department of Energy through Contract No. DE-FG02-96ER40983, DE-FG05-88ER40407, and DE-FG05-88ER40330, respectively. Oak Ridge National Laboratory is managed by Lockheed Martin Energy Research Corporation under contract DE-AC05-96OR22464 with the U. S. Department of Energy. UNIRIB is a

consortium of universities, State of Tennessee, Oak Ridge Associated Universities, and Oak Ridge National Laboratory. The Joint Institute for Heavy Ion Research has as member institutions the University of Tennessee, Vanderbilt University, and Oak Ridge National Laboratory; it is supported by the three members and the U. S. Department of Energy.

### References

1. S. Hofmann, W. Reisdorf, G. Münzenberg, F. P. Hessberger, J. R. H. Schneider, and P. Armbruster, *Z. Phys.* **A305**, 111 (1982).
2. P. J. Sellin, P. J. Woods, D. Branford, T. Davinson, N. J. Davis, D. G. Ireland, K. Livingston, R. D. Page, A. C. Shotter, S. Hofmann, R. A. Hunt, A. N. James, M. A. C. Hotchkis, M. A. Freer, and S. L. Thomas, *Nucl. Instrum. Methods Phys. Res. A* **311**, 217 (1992).
3. T. N. Ginter, Article in the Present Volume (1999).
4. K. P. Jackson, C. U. Cardinal, H. C. Evans, N. A. Jelley, and J. Cerny, *Phys. Lett.* **33B**, 281 (1970).
5. P. J. Woods and C. N. Davids, *Annu. Rev. Nucl. Part. Sci.* **47**, 541 (1997).
6. J. C. Batchelder, C. R. Bingham, K. Rykaczewski, K. S. Toth, T. Davinson, J. A. McKenzie, P. J. Woods, T. N. Ginter, C. J. Gross, J. W. McConnell, E. F. Zganjar, J. H. Hamilton, W. B. Walters, C. Baktash, J. Greene, J. F. Mas, W. T. Milner, S. D. Paul, D. Shapira, X. J. Xu, and C. H. Yu, *Phys. Rev C* **57**, R1042 (1998).
7. C. N. Davids, P. J. Woods, D. Seweryniak, A. A. Sonzogni, J. C. Batchelder, C. R. Bingham, T. Davinson, D. J. Henderson, R. J. Irvine, G. L. Poli, J. Uusitalo, and W. B. Walters, *Phys. Rev. Lett.* **80**, 1849 (1998).
8. S. Hofmann, in *Nuclear Decay Models*, edited by D. N. Poenaru, Inst. of Phys. Publishing, Bristol and Philadelphia, 1996, pp. 143-203.
9. F. D. Becchetti, Jr. and G. W. Greenlees, *Phys. Rev.* **182**, 1190 (1969).
10. P. Möller, J. R. Nix, W. D. Myers, and W. J. Swiatecki, *At. Data Nucl. Data Tables* **59**, 185 (1995).
11. S. Åberg, P. B. Semmes, and W. Nazarewicz, *Phys. Rev. C* **56**, 1762 (1997).
12. S. A. Gurvitz and G. Kalbermann, *Phys. Rev. Lett.* **59**, 262 (1987).
13. S. A. Gurvitz, *Phys. Rev. A* **38**, 1747 (1988).